JOURNAL OF MATERIALS SCIENCE 29 (1994) 2406–2416

How the work of adhesion affects the mechanical properties of silica-filled polymer composites

S. W. SHANG*, J. W. WILLIAMS, K-J. M. SÖDERHOLM‡
Departments of Materials Science and Engineering, and ‡Dental Biomaterials, University of Florida, Gainesville, FL 32611, USA

An equation correlating work of adhesion (W_a) with Young's modulus and tensile strength of silica-filled polymer composites is derived. It shows that the logarithms of Young's modulus and tensile strength are inversely proportional to W_a. Fourier transform infrared (FT. i.r.) results of the composites show that the silica interphase thickness increases with increased W_a^h values (the hydrogen bond component of W_a). The logarithmic correlation between interphase thickness and W_a is similar to that found for both Young's modulus and tensile strength. These similarities suggest that W_a can be used to quantify interfacial bonding. Our study further shows that the composite with the lowest W_a value follows the Guth–Smallwood equation for predicting Young's modulus. However, as the interphase layer becomes thicker (increased W_a value), Young's modulus increases more than predicted from the Guth–Smallwood equation. Thus, an extension of the Guth–Smallwood equation is introduced to account for the effect of W_a on the Young's modulus value.

1. Introduction

Extensive work has been done to correlate mechanical properties of composites with the strength of the interfacial bonds [1–38]. These interfacial bonds are often described as being good or poor. Early studies concluded that the strength of composites is maximized when the interfacial bond between the filler surface and the polymer matrix is optimized [1–12, 18–33].

Interfacial bond strength can be determined from fibre pull-out studies. However, the complex shape of particulate filler particles makes such model studies of fibres questionable (39). Consequently, very few studies have quantitatively correlated the mechanical properties of particulate filled composites with their interfacial bond strength values [1–4, 32]. However, without a quantitative approach, the nature of the interfacial bond cannot be fully understood. To quantify the interfacial bond strength, it is hypothesized that the mechanical properties of particulate filled composites can be correlated with the work of adhesion (W_a) values of their filler particles. The rational for this hypothesis is that in several silica-filled polymer composites, inter-molecular forces exist between the silanol groups of the silica filler and the carbonyl groups of the polymer matrix [1, 32]. Separating these molecules requires that a certain work is done. This work is the work of adhesion (W_a) and its detailed computation has been given elsewhere [1, 32].

The main objective of this study is to test the hypothesis that the W_a values can be used to predict the strength properties of composites. To do that, the first objective is to correlate the work of adhesion with the mechanical properties of a filled polymer. Such correlations will be determined by plotting both Young's modulus and the tensile strength values of silica-filled composites as functions of W_a. The success of these correlations will be used to test the validity of the proposed hypothesis. The second objective is to determine whether the thickness of the composite interphase correlates with W_a. Such a correlation is expected, since a stronger filler–polymer interaction should result in more molecular interactions and a thicker interphase. A thicker interphase layer, reflected in a higher W_a value, would facilitate the formation of interpenetrating networks. The interpenetrating network would enhance the strength properties and support our hypothesis that there are correlations between W_a, interphase thickness and the strength properties.

2. Experimental procedure

2.1. Materials

Spherical silica particles, 0.6 or 0.014 μm in diameter, were used as fillers in an ethylene–vinyl acetate (E–Va) copolymer (72 wt % ethylene and 28 wt % vinyl acetate). The 0.6 μm silica particles were prepared according to the method described by Stöber *et al.* and Tai *et al.* [40, 41]. The fine MS-7 grade fused silica (0.014 μm) was obtained from Cab-o-sil Division (Cabot Corporation).

* *Present address*: Baxter Healthcare Corporation, Round Lake, IL 60073, USA

0022–2461

2.2. Surface treatment

Amorphous fused quartz plates were used as a model filler to characterize the surface properties of silica [42]. The properties of the plates were assumed to be similar to the surface properties of the silica filler particles. Two surface treatment procedures were used to modify the silica particles or the quartz plates. They were: (a) heat, and (2) heat combined with trimethylchlorosilane, $[(CH_3)_3 - SiCl]$ (TMCS), treatments [1, 32, 42].

2.3. Determination of work of adhesion

Work of adhesion (W_a) was determined to quantify the interfacial bond strength between the silica surface and the E–Va copolymer matrix, and where W_a was written as [1, 20, 24, 26–28, 32]:

$$W_a = W_a^d + W_a^h \quad (1)$$

In Equation 1, W_a^d represents dispersion forces and W_a^h hydrogen bonds and polar forces [20, 24, 26–28].

The W_a^d value was determined from the dispersion component of the surface energies of both the filler (τ_f^d) and the polymer (τ_p^d).

$$W_a^d = 2(\tau_f^d \tau_p^d)^{1/2} \quad (2)$$

The τ_f^d and τ_p^d values were determined from Owens' equation [43],

$$1 + \cos\theta = 2(\tau_s^d)^{1/2}(\tau_l^{d\,1/2}/\tau_l) + 2(\tau_s^h)^{1/2}(\tau_l^{h\,1/2}/\tau_l) \quad (3)$$

by contact angle measurements. l represents a liquid, and s a solid. Thus, contact angle values of water and iodine on surfaces of either quartz plates (simulating the silica filler) or E–Va copolymer blocks (simulating the polymer matrix) were used in Equation 3 to calculate τ_s^d, that could be either τ_f^d of the quartz or the τ_p^d of the E–Va polymer.

The W_a^h of surfaces with poor interfacial bonding was determined by

$$W_a^h = 2(\tau_f^h \tau_p^h)^{1/2} \quad (4)$$

while the W_a^h of surfaces with strong hydrogen and polar bonds was determined from Fowkes's equation [1, 27, 28, 32]. This equation is written as:

$$W_a^h = f \cdot \Delta H^{ab} \text{ moles of acid–base pairs/unit area} \quad (5)$$

$$\Delta H^{ab}(\text{kJ mol}^{-1}) = 1.00\ \Delta v(\text{kJ mole}^{-1}/\text{cm}^{-1}) \quad (6)$$

where ΔH^{ab} is equal to 8.3 kcal mol^{-1} of acid–base pairs, and Δv is the peak shift seen in the i.r. spectrum due to hydrogen bond formation.

2.4. Determination of surface characteristics

The surface properties were measured with a contact angle goniometer. In addition, the number of hydroxyl groups present on the silica powder surfaces [44–46] was determined by titration with *n*-butylamine consisting of 0.1 M *n*-butylamine dissolved in benzene [47–49]. To determine the equilibrium value between the hydroxyl groups and the amine group, an indicator dye was added. This indicator dye consisting of 1.5 g neutral red dissolved in 40 ml benzene. To determine the equilibrium value, samples containing different amounts of the *n*-butylamine were prepared [47–49]. The indicator dye was added to these samples. The two sample concentrations where one could identify a change from a constant colour to a colour change represented the equilibrium value.

2.5. Polymer adsorption on silica surface

It was assumed that the quantity of polymer adsorbed on the silica surface from the polymer solution would simulate the composite interphase thickness. Based on that assumption, we quantified the interphase thickness by measuring the amount of polymer adsorbed on the silica filler surfaces.

The amount of polymer bonded and/or adsorbed on silica [50–54] was determined with a Nicolet 60SX Fourier transform infrared (FT–i.r.) spectrometer equipped with a mercury–cadmium–telluride (MCT) detector. A diffuse reflectance accessory (Model DRA-3SO) was used during spectra collection. During these collections, KBr powder was used both as a reference powder and as a medium with which silica powder was mixed [55–64]. The diffuse reflectance infrared Fourier transform (DRIFT) spectra [55, 60, 61] were acquired at a nominal resolution of 4 cm^{-1}. From the DRIFT spectra the amount of hydrogen bonding and interaction energy between the silanol groups of the silica filler and the carbonyl groups of the polymer could be determined [1, 32].

Both the heat and heat/TMCS surface modified Cab–O–Sil silica particles [65–70] and their ability to absorb polymer [53, 54] were studied. This was done by preparing different (0.5–6.0%) volume concentrations of E–Va dissolved in benzene and letting 100 ml of these solutions adsorb onto 0.3 g Cab–O–Sil silica powder. During the absorption period, the silica powders were stirred in the polymer solution for 1 h. The polymer-absorbed silica particles were then centrifuged for 5 min at 5000 r.p.m. and dried in air.

The quantity of E–Va adsorbed on the silica was determined by DRIFT. This determination was done by first relating the amount of silica to the intensity of the siloxane (Si–O) peak at 1100 cm^{-1} [65, 66]. The quantity of the adsorbed E–Va could then be determined from carbonyl peaks (both hydrogen and non-hydrogen bonded C=O groups). The peak at 1739 cm^{-1} was assigned to non-hydrogen bonded C=O, while hydrogen bonded C=O has a peak at 1704 cm^{-1} [27, 28, 71]. The integrated peak ratio (C=O versus Si–O) was used to determine the quantity polymer adsorbed per unit area silica surface. Even though this only provides the relative amount of polymer adsorbed onto silica surfaces, the amount of polymer could be determined as the amount of silica powder was known.

To characterize E–Va, the E–Va was first dissolved in benzene. One drop of the E–Va solution was added to the KBr in the sample cup of the DRIFT. The E–Va carbonyl (C=O) peak was recorded after the solvent had evaporated.

2.6. Ratio of hydrogen bonded to non-hydrogen bonded carbonyl group

The ratio of hydrogen bonded C=O to non-hydrogen bonded C=O peaks was determined, and the original overlapped peaks of 1739 and 1704 cm^{-1} were deconvoluted. Each deconvoluted peak area was then integrated by the Nicolet software.

2.7. Composite sample preparation and mechanical testing.

E–Va composites of different volume fraction fillers (1, 3, 5, 10, 15 and 20%) were cast from benzene/E–Va solutions. Dumb-bell shaped tensile specimens were prepared according to ASTM specification 1822 from compression moulded composite sheets. The composite specimens were first annealed to 100 °C for 3 h, and then conditioned at 25 °C for 3 days before they were tested in tension. The testing procedure was conducted at 25 °C by using an Instron testing machine Model 1122 and a crosshead speed of 50.8 mm/min (2 in/min). At least six specimens per group were tested. The tensile strength and Young's modulus were determined from the charts.

2.8. Tensile fracture surface studies

Scanning electron microscopy (SEM) was used to study the morphology of the fractured composite samples. The matrix and the Stöber silica particle interface, either heat or heat/TMCS treated, were examined by SEM.

3. Results and discussion

3.1. Effect of silica particle size and volume fraction on Young's modulus

Figs 1 and 2 show Young's moduli of composites, E, containing Stöber silica and Cab–O–Sil silica versus silica filler volume fraction, respectively. The composites had a higher Young's modulus than the unfilled E–Va copolymer matrix. The modulus increased with increased silica fraction. The heat treated silica composites had higher Young's moduli than the heat/TMCS treated silica composites. For identical filler volumes, the Cab–O–Sil composites were stronger than the Stöber silica containing composites. Since Cab–O–Sil consists of smaller silica particles than the Stöber silica, Cab–O–Sil silica has more surface area available to bond and adsorb polymer for a given filler volume. These bonded and adsorbed polymer chains become stiff due to loss of their flexibility. The increased number of stiffened molecules explains why the Cab–O–Sil composites had higher Young's modulus than the Stöber composites. Consequently, smaller filler particles result in better reinforcing ability.

3.2. Effect of silica particle size and volume fraction on tensile strength

Figs 3 and 4 show the tensile strength of composites, σ_c, containing Stöber silica and Cab–O–Sil silica versus filler volume fraction. The Stöber composites had a lower tensile strength than the unfilled E–Va copolymer, suggesting that Stöber silica weakened the composite [1]. In contrast, the Cab–O–Sil composites were stronger than the unfilled polymer, at least as long as the filler fraction did not exceed 15% silica. At lower Cab–O–Si filler fractions, the tensile strength of the composite increased with increased silica volume, reaching a maximum around 4 vol % filler [1]. Composites containing heat treated silica had higher tensile strength than those containing heat/TMCS treated silica.

As a general finding, the larger Stöber silica particles were less effective as a reinforcing filler than the finer Cab–O–Sil filler. These conclusions are in line with other findings suggesting that the reinforcing ability often decreases with an increase in filler particle size [72–74].

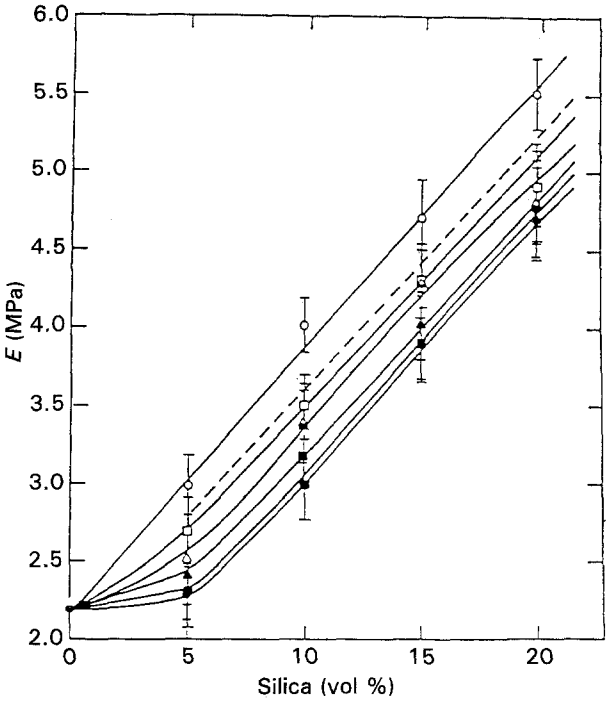

Figure 1 Effect of volume fraction and surface properties of Stöber silica filler on Young's modulus, E, of polymer composites. Surface treatment: (○) 110 °C, (□) 500 °C, (△) 750 °C, (▲) 750 °C/TMCS, (■) 500 °C/TMCS, (●) 110 °C/TMCS. Diameter of Stöber silica, 0.6 μm.

3.3. Work of adhesion

Fig. 5 shows the values of work of adhesion (W_a) for different silica/E–Va interfaces. These values include the ratio of the hydrogen component, W_a^h, to the dispersion component of work of adhesion, W_a^d [1, 32]. From Fig. 5 it is seen that Stöber silica had a slightly higher W_a^h than Cab–O–Sil silica. This can be explained from earlier studies which showed that Stöber silica has more hydroxyl groups per unit are a silica surface [1, 32]. In addition, heat treated silica had a higher W_a than heat/TMCS treated silica. Heating to 110, 500 and 750 °C reduced the number of hydroxyl groups present on the silica surface. Fig. 6 confirms this by comparing contact angle measurements of water on quartz plates. The contact angle

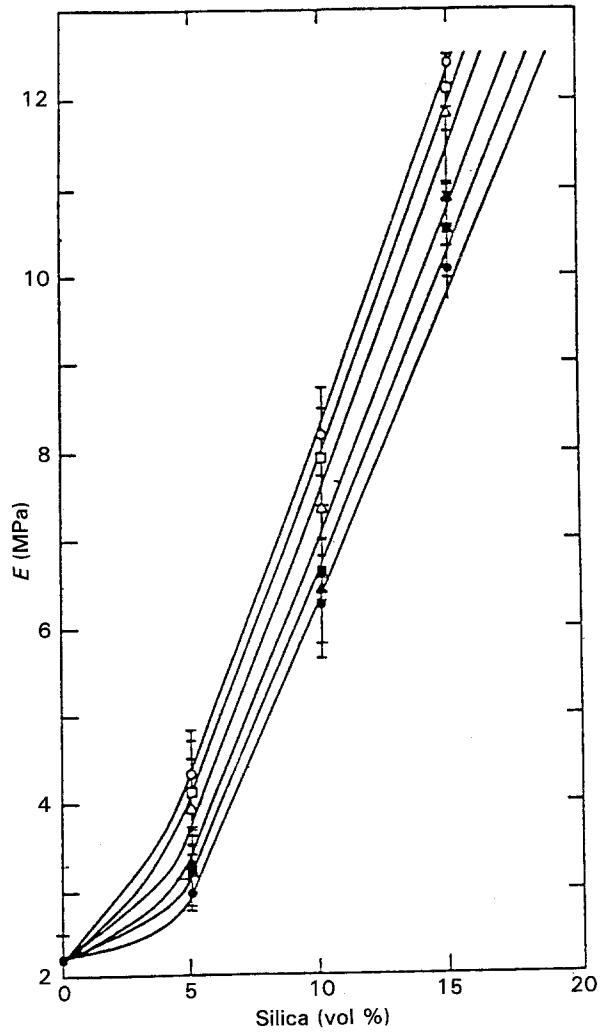

Figure 2 Effect of volume fraction and surface properties of Cab–O–Sil silica filler on Young's modulus, E, of polymer composites. Surface treatment: (○) 110 °C, (□) 500 °C, (△) 750 °C, (▲) 750 °C/TMCS, (■) 500 °C/TMCS, (●) 110 °C/TMCS. Diameter of Cab–O–Sil silica, 0.014 μm.

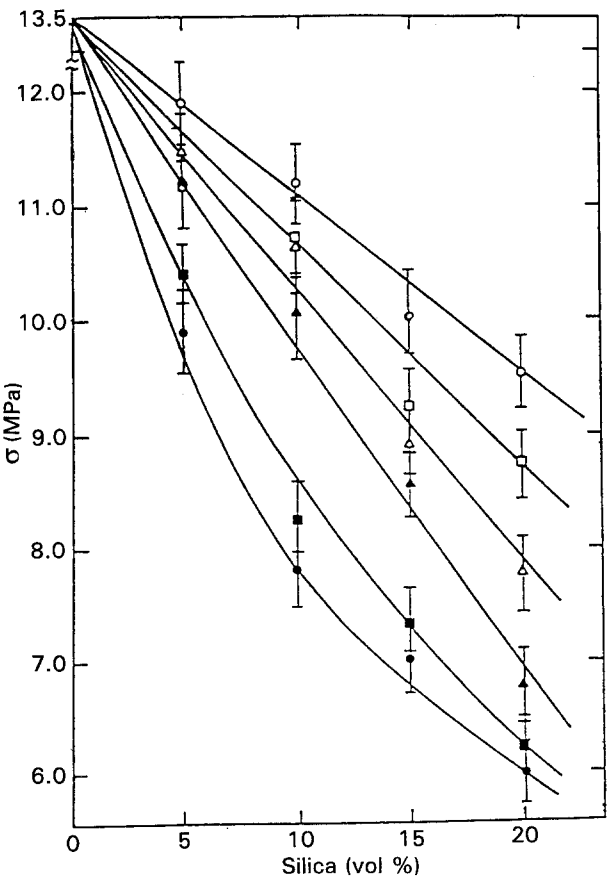

Figure 3 Effect of volume fraction and surface properties of Stöber silica filler on the tensile strength, σ_c, of polymer composites. Surface treatment: (○) 110 °C, (□) 500 °C, (△) 750 °C, (▲) 750 °C/TMCS, (■) 500 °C/TMCS, (●) 110 °C/TMCS. Diameter of Stöber silica, 0.6 μm.

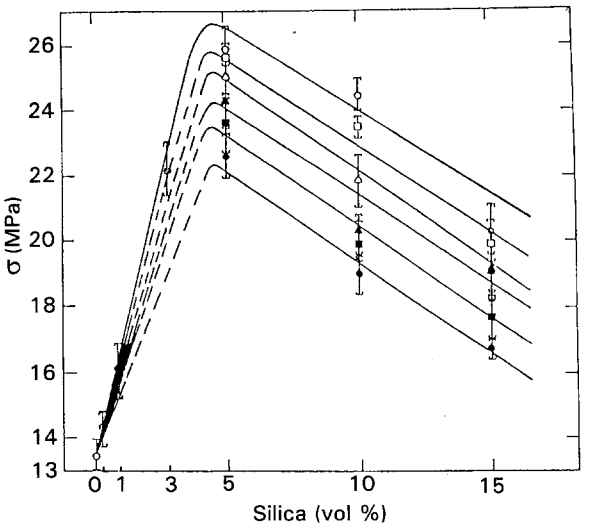

Figure 4 Effect of volume fraction and surface properties of Cab–O–Sil MS-7 Silica filler on the tensile strength, σ_c, of polymer composites. Surface treatment: (○) 110 °C, (□) 500 °C, (△) 750 °C, (▲) 750 °C/TMCS, (■) 500 °C/TMCS, (●) 110 °C/TMCS. Diameter of Cab–O–Sil silica, 0.014 (μm.

values increased as the quartz plates were heated at higher temperatures. The change of W_a mainly comes from the variation in the W_a^h. The W_a^h increased with an increase in silica surface hydroxyl groups [1, 32].

Only a limited number of hydroxyl groups existed after the silica surface had been heated to 110, 500 or 750 °C and then treated with TMCS [1, 32]. Fig. 6 shows that the heat/TMCS treated quartz had a higher contact angle value than the heated quartz. This suggests that the silica surface changes from being hydrophilic to become hydrophobic when it is heated and TMCS treated. The W_a^h values also contributed less to the W_a values than the W_a^d values did.

3.4. Effect of W_a on Young's modulus

After the silica/E–Va interface is quantified in terms of W_a, the effect of W_a on Young's modulus and the tensile strength of these composites could be determined.

3.4.1. Young's modulus

In Fig. 7, Young's moduli (log E) of Cab–O–Sil and Stöber composites are plotted against the reciprocal of W_a ($1000/W_a$) in a semi-logarithmic co-ordinate system. This figure shows an exponential relationship between log E and W_a^{-1} at a given volume fraction silica, and that Young's modulus of a silica composite increases as W_a increases. The results depicted in Fig.

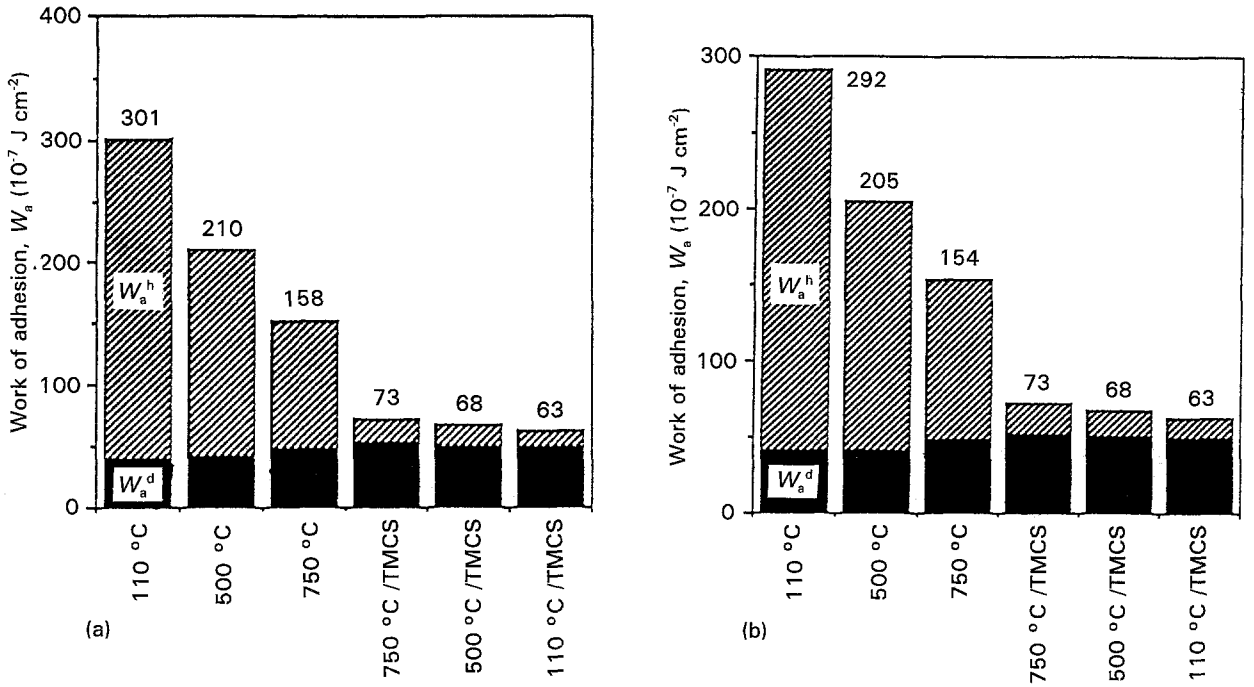

Figure 5 Calculated work of adhesion, $W_a = W_a^d + W_a^h$, at different silica/E–Va interfaces: (a) stöber silica/E–Va composites, (b) Cab–O–Sil/E–Va composites.

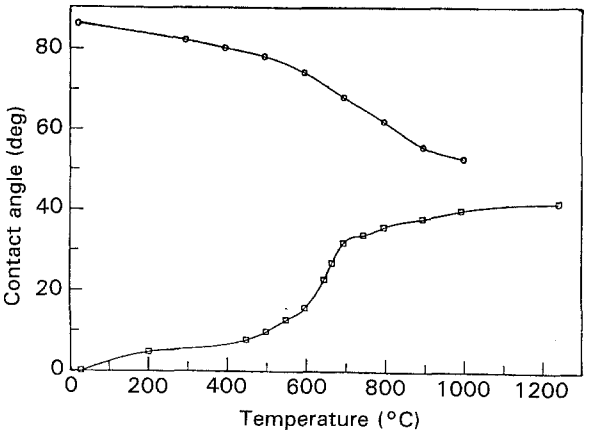

Figure 6 Contact angles of water on the surfaces of the fused quartz plates treated by heat(○) or heat/TMCS(□).

7 can be written as:

$$E_c = C\exp[-K_{E_c}(1/W_a)] \quad (7)$$

where E_c is the modulus of the composite, and C and K_{E_c} are constants. The K_{E_c} term represents the slope of log E_c versus W_a^{-1} and is determined from the experimental data.

3.4.2. Quantitative relationship of Young's modulus

For the same volume fraction silica, but where the different fillers have different silica surface properties, the constant C in Equation 7 can be deleted and the ratio of two moduli written as:

$$\frac{E_c}{E_{co}} = \exp\{-K_{E_c}[(1/W_a) - (1/W_{ao})]\} \quad (8)$$

where E_{co} is the modulus of the silica composite with the weakest interfacial bond (110 °C/TMCS treatment, $W_{ao} = 63 \times 10^{-7}$ J cm^{-2}). The W_{ao} is the work of adhesion of the material with the weakest interfacial bond. When Young's modulus of a composite with its corresponding W_a is known, Equation 8 can be used to predict Young's modulus of another composite with another W_a but with the same silica content.

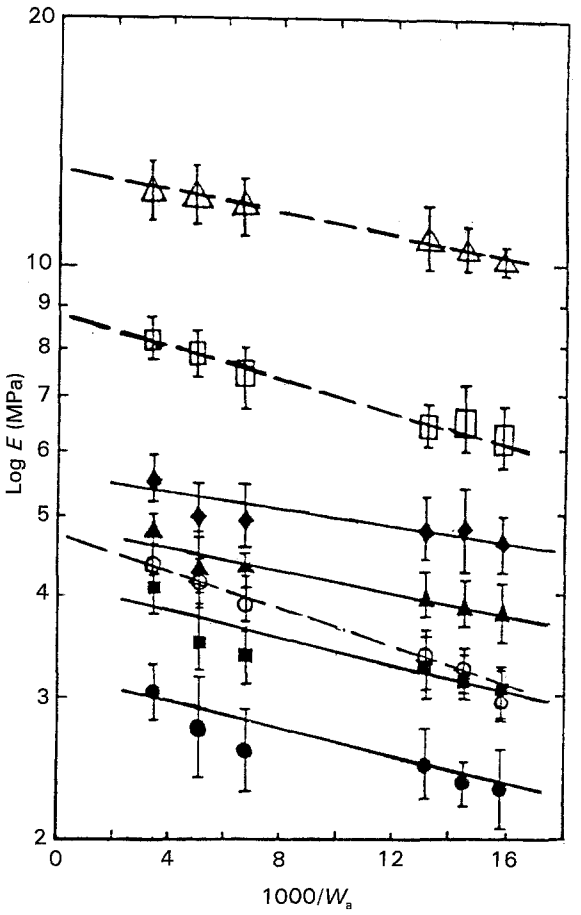

Figure 7 Effect of work of adhesion, W_a, on Young's modulus, log E, of polymer composites containing different silica particle sizes and volume fractions. MS-7 grade silica. (△) 15 vol %, (□) 10 vol % (○) 5 vol %. 0.6 μm silica: (◆) 20 vol %, (▲) 15 vol %, (■) 10 vol %, (●) 5 vol %.

Table I shows the K_{E_c} values of Stöber and Cab–O–Sil silica composites with different silica contents. This table shows that the K_{E_c} value is independent of volume fraction silica. The Cab–O–Sil composites have a higher K_{E_c} value than the Stöber composites. These K_{E_c} values show how Young's modulus changes with W_a^{-1}. Since the K_{E_c} value is a function of silica particle size, the change in K_{E_c} with particle size change proves that the effect of the interfacial bond on Young's modulus depends on filler particle size.

3.4.3. Extension of Guth–Smallwood equation

For composites containing Stöber silica, Young's modulus of the composite with the weakest interfacial bond (the 110 °C/TMCS composite) followed the Guth–Smallwood equation [15, 16]:

$$E_{110\,°C/TMCS} = E_p(1 + 2.5\,V_f + 14.1\,V_f^2) \quad (9)$$

In Equation 9, $E_{110\,°C/TMCS}$ is the modulus of that composite, which is equivalent to the E_{co} in Equation 8. E_p is the modulus of the unfilled E–Va copolymer. V_f is the volume fraction Stöber silica. Equation 8 can be combined with Equation 9 to yield:

$$E_c = E_p(1 + 2.5\,V_f + 14.1\,V_f^2) \times \exp\{-K_{E_c}[(1/W_a) - (1/W_{ao})]\} \quad (10)$$

Equation 10 then becomes an extension of the Guth–Smallwood equation accounting for the effect of W_a on Young's modulus. At a given V_f, Young's modulus of Stöber silica composites increases as W_a increases.

Equation 10 predicts the modulus of the Stöber composites tested for the different experimental conditions. Good agreements are obtained for all values of W_a and V_f calculated from Equation 10, except for the case with the highest interfacial bond ($W_a = 301 \times 10^{-7}$ J cm^{-2}). The predicted modulus value for the latter case is lower than the experimentally obtained value. Guth–Smallwood's equation correctly predicts the relatively modest increases in modulus caused by the addition of inactive or non-reinforcing fillers. However, the Guth–Smallwood equation is relatively unreliable for predicting highly reinforced systems [31]. Therefore, for composites containing Cab–O–Sil silica, Equation 10 cannot be applied; however, Equation 8 gave good agreements for all composites.

3.5. Effect of W_a on tensile strength

Fig. 8 shows that the tensile strengths (log σ) of Cab–O–Sil and Stöber composites can be plotted against $1000/W_a$ in a semi-logarithm co-ordinate system. The correlation is similar to that obtained for Young's modulus (Equation 7), in that an exponential relationship exists between log σ and W_a^{-1}. The tensile strengths of silica composites increased as W_a increased, which can be expressed as:

$$\frac{\sigma_c}{\sigma_{co}} = \exp\{-K_{\sigma_c}[(1/W_a) - (1/W_{ao})]\} \quad (11)$$

where σ_c is the tensile strength of a silica composite having W_a at the interface. The σ_{co} is the tensile strength of the silica composite having the weakest interfacial bond (110 °C/TMCS treatment, $W_{ao} = 63 \times 10^{-7}$ J cm^{-2}). The W_{ao} is the work of adhesion of the weakest interfacial bond. When the tensile strength of a composite and its corresponding W_a is known, Equation 11 can predict the tensile strength of silica containing composites of a certain V_f, but where the fillers have different W_a values.

The K_{σ_c} in Equation 11 is the slope of log σ versus W_a^{-1}. Table II shows the values of K_{σ_c}. The K_{σ_c} value depends on both silica particle size and volume fraction. At a given volume fraction silica, the Stöber composite had a higher K_{σ_c} value than the Cab–O–Sil composite. The K_{σ_c} values increased as silica content increased, especially for the Stöber silica composites. This suggests that for the tensile strengths of silica composites, the interfacial bond strength has a more

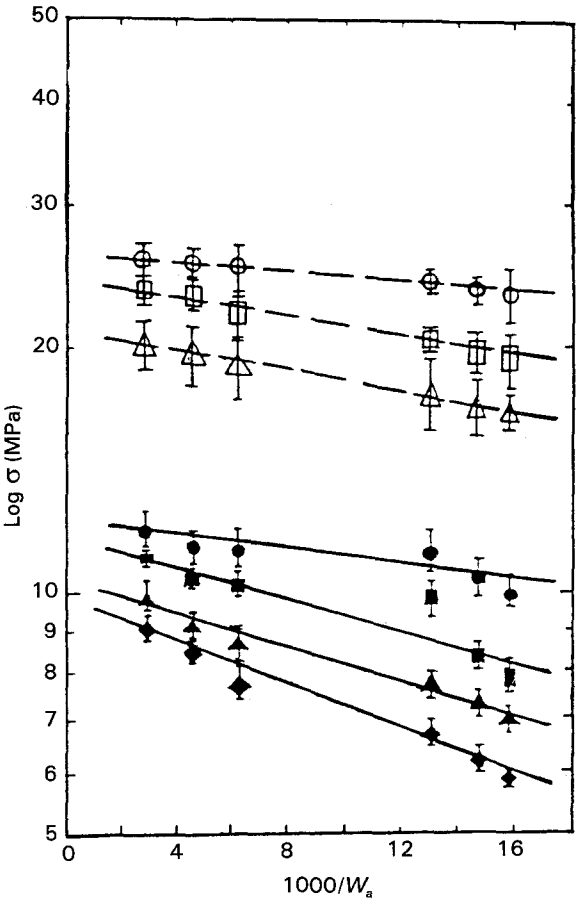

Figure 8 Effect of work of adhesion, W_a, on the tensile strength of polymer composites, log σ_c, containing different silica particle sizes and volume fractions. MS-7 grade silica: (○) 5 vol %, (□) 10 vol % , (△) 15 vol %. 0.6 μm silica: (●) 5 vol %, (■) 10 vol %, (▲) 15 vol %, (◆) 20 vol %.

TABLE I Slope ($K_{E_c} \times 1000$, 10^{-7} J cm^{-2}) of Young's modulus versus W_a^{-1} of silica-filled composites

Silica (vol %)	Stöber silica	Cab–O–Sil silica
5	7.6	10.8
10	7.9	10.7
15	7.1	10.3
20	7.2	–

TABLE II Slope ($K_{\sigma_c} \times 1000$, 10^{-7} J cm^{-2}) of Tensile strength versus W_a^{-1} of silica-filled composites

Silica (vol %)	Stöber silica	Cab–O–Sil silica
5	6.4	4.6
10	9.6	6.1
15	12.1	7.3
20	14.2	–

pronounced effect on the Stöber composites than on the Cab–O–Sil composites.

3.6. SEM micrograph of the tensile fracture surface

Fig 9a and 10a show the tensile fracture surfaces of a composite containing 5% filler preheated to 110 °C, and another composite containing 15% filler preheated to 750 °C, respectively. These SEM micrographs show that most Stöber silica particles remain embedded in the polymer matrix after fracture. These composites are examples of good interfacial filler bonding. In contrast, Fig. 9b shows the fractured surface of a composite containing a 110 °C/TMCS treated silica filler, while Fig. 10b shows a composite containing a 750 °C/TMCS treated silica filler. These composites are examples of materials with weak interfacial bonding. The Stöber silica particles are nearly free from polymer matrix. From these SEM micrographs, it can be concluded that the silica surface properties strongly influence the interfacial bond strength.

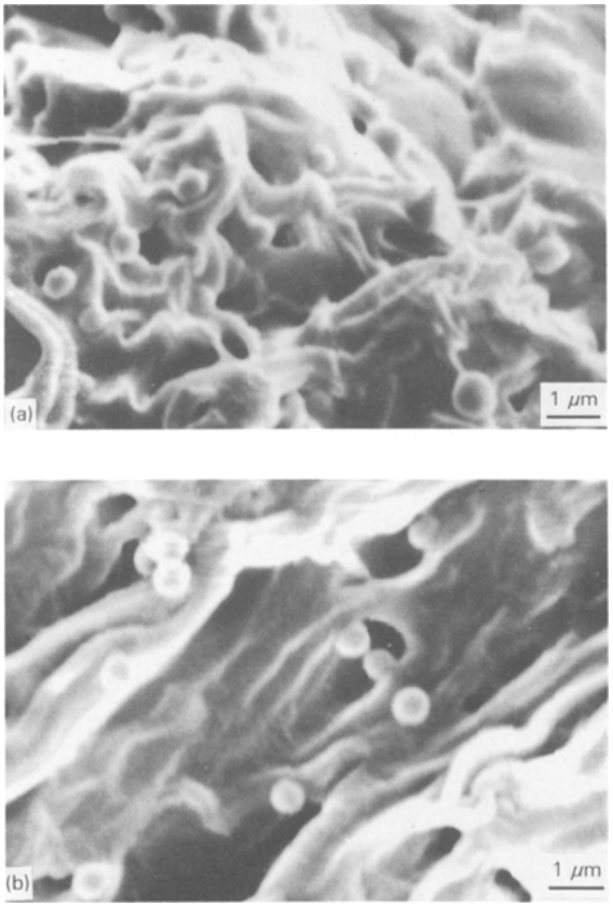

Figure 9 SEM micrograph of the tensile fracture surface of 5 vol % Stöber silica fillers in E–Va matrix. Silica treatment at: (a) 100 °C, (b) 110 °C/TMCS.

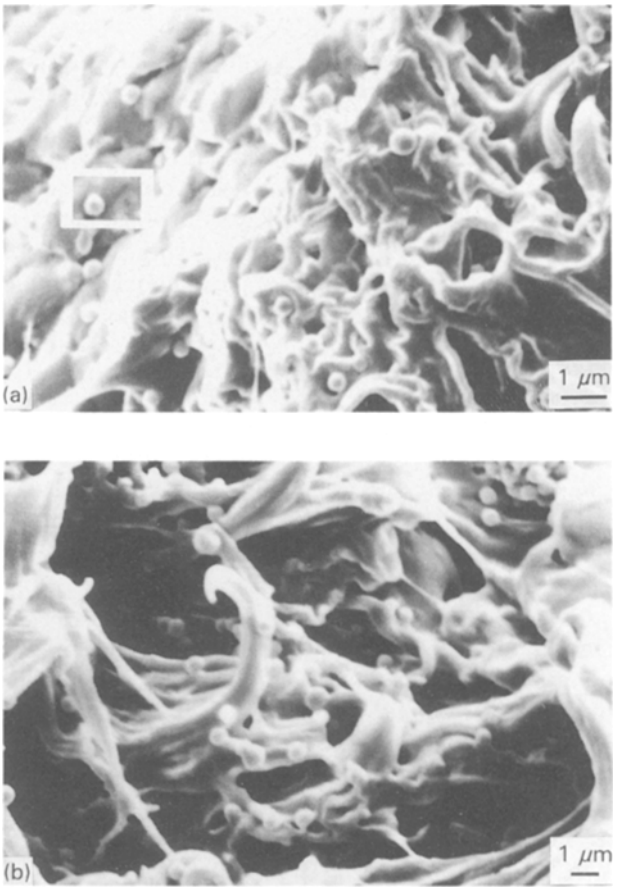

Figure 10 SEM micrograph of the tensile fracture surface of 15 vol % Stöber silica fillers in E–Va matrix. Silica treatment at: (a) 750 °C, (b) 750 °C/TMCS.

3.7. Hydrogen bonds at the interface

Fig. 11 shows the FTIR spectra of 110 and 750 °C/TMCS treated silica, on which E–Va polymer is bonded and/or absorbed. The spectra have two carbonyl group (C=O) peaks. One is at 1739 cm^{-1}, and the other is at 1704 cm^{-1}. Spectrum A shows the C=O peak at the E–Va copolymer at 1739 cm^{-1}. Spectrum B shows E–Va bonded and absorbed on the 750 °C/TMCS treated silica surface, and where the C=O group shows up as a small peak at 1704 cm^{-1} and a large peak at 1739 cm^{-1}. Spectrum C shows how the C=O group of E–Va is absorbed on silica preheated to 110 °C as both a large peak at 1704 cm^{-1} and a small peak at 1739 cm^{-1}.

When hydrogen bonds form between the C=O groups of E–Va and the isolated hydroxyl groups of the silica surface, the C=O peak shifts from 1739 to 1704 cm^{-1} (27, 28, 71). Fig. 5 shows that the heat treated silica interface has a higher W_a^h value than the heat/TMCS treated silica. A higher W_a^h is due to more hydrogen bonds at the silica/E–Va interface. Thus, the hydrogen bond density at the interface is the dominant component that determines the interfacial bond strength.

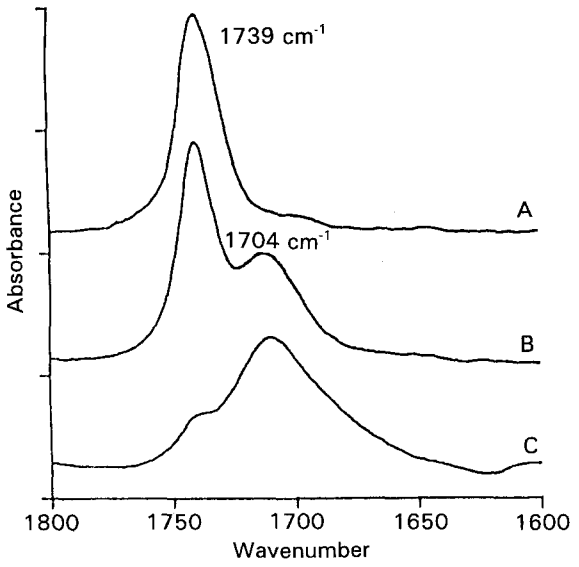

Figure 11 FT–i.r. spectra of E–Va bonded and adsorbed on different Cab–O–Sil silica surfaces. The C–O shift to a low wave number as hydrogen bond formed at the interface. (A) pure E–Va copolymer, (B) E–Va absorbed on to silica with 750 °C/TMCS treatment, (C) E–Va absorbed onto silica with 110 °C treatment.

3.8. Polymer adsorption onto silica surface from various polymer concentrations

Fig. 12 shows FT–i.r. spectra of E–Va bonded and adsorbed onto both 110 and 750 °C/TMCS treated silica from either 0.56, 0.8 or 4.2% polymer solutions. Changes in peak intensity of C=O at 1704 and 1739 cm^{-1} are shown, and relate to variations in either silica surface properties or polymer solution concentrations.

The isolated hydroxyl group of silica [65–70], shown as a peak at 3747 cm^{-1}, is responsible for forming hydrogen bonds with the E–Va carbonyl group. In Fig. 12, the first three spectra show the E–Va adsorbed onto 110 °C treated silica from 0.56, 0.8, and 4.3% polymer solutions, respectively. The 0.56% (A) spectrum (Fig. 12) shows a large peak at 1704 cm^{-1}, and a very small peak at 1739 cm^{-1}. Due to less C=O (i.e. E–Va) available to bond to the silica surface, the isolated hydroxyl peaks at 3747 cm^{-1} still remain. However, when more E–Va polymer molecules are available, as in the 4.2% (A) spectrum (Fig. 12), more hydrogen bonds form at the interface shown by the disappearance of the isolated hydroxyl group peak. Also, due to the increased C=O concentration, some C=O groups become unable to form hydrogen bonds, shown by an increase in the non-hydrogen bonded C=O peak at 1739 cm^{-1}.

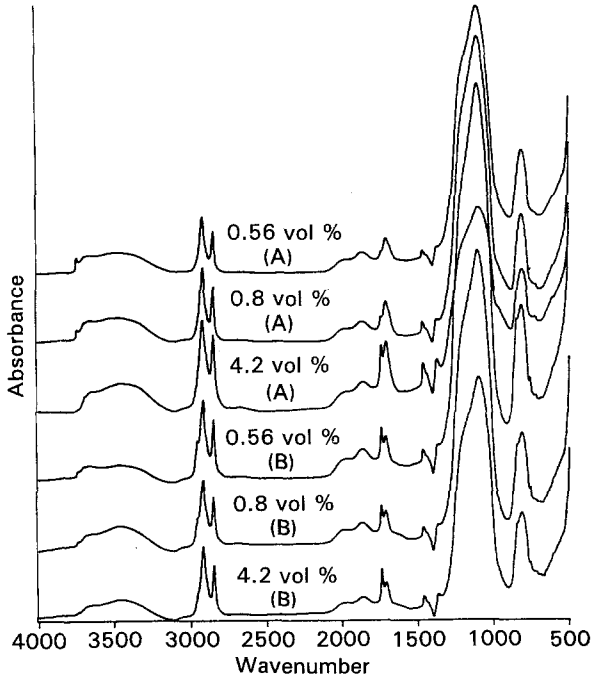

Figure 12 FT–i.r. spectra of E–Va bonded and adsorbed from different polymer concentrations on (A) 110 °C, (B) 750 °C/TMCS Cab–O–Sil silica surfaces.

Table III shows the relative amount of polymer bonded and adsorbed to the silica surface. The amount of E–Va polymer bonded and adsorbed per unit surface area of silica was determined from the C=O and Si–O peaks. Table III shows that the C=O/Si–O ratio increased with an increase in polymer concentration. Also, 110 °C treated silica had a higher C=O/Si–O ratio than 750 °C/TMCS treated silica.

Figs 13 and 14 show the magnified peak intensities of hydrogen to non-hydrogen bonded C=O groups, previously shown in Fig. 12. Fig. 13 shows the 110 °C treated silica, where the hydrogen bonded C=O peak is plotted at a fixed peak intensity. Fig. 14 shows the 750 °C/TMCS treated silica spectra, where the non-hydrogen bonded C=O peak is plotted at a fixed peak intensity.

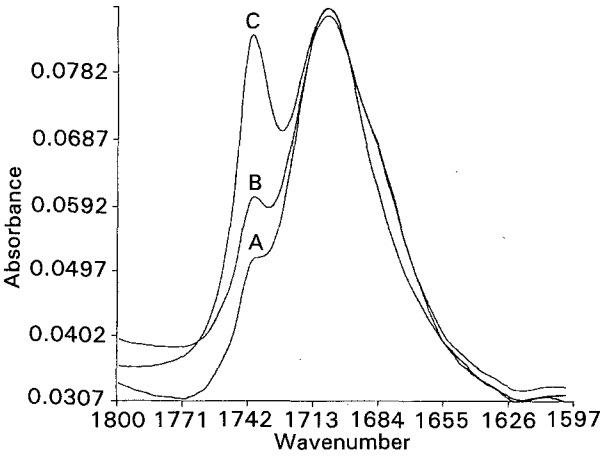

Figure 13 FT–i.r. spectra of magnified peak intensity of hydrogen and non-hydrogen bonded carbonyl groups of E–Va on the 110 °C treated silica in Fig. 12. (A) 0.56 vol %, (B) 0.8 vol %, (C) 4.2 vol %.

TABLE III Relative amount of E–Va bonded/adsorbed onto silica (C–O/Si–O) per unit area silica surface

Polymer solution concentration (vol %)	Silica treatment	
	110 °C	750 °C/TMCS
0.56[a]	0.025	0.019
0.80	0.030	0.021
4.20[b]	0.086	0.054

[a] Thin coating of E–Va on silica surface.
[b] Thick coating of E–Va on silica surface.

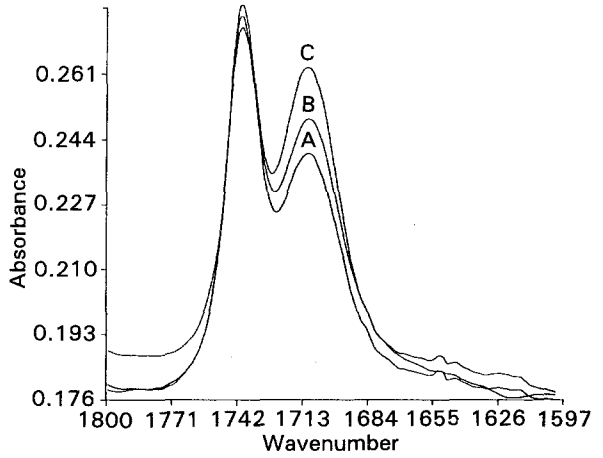

Figure 14 FT-i.r. spectra of magnified peak intensity of hydrogen and non-hydrogen bonded carbonyl groups of E–Va on the 750 °C/TMCS treated silica in Fig. 12. (A) 4.2 vol %, (B) 0.8 vol %, (C) 0.56 vol %.

Table IV shows the integrated peak intensity ratio of hydrogen bonded to non-hydrogen bonded C=O. The ratio was measured from the deconvoluted peaks of hydrogen bonded groups to non-hydrogen bonded C=O groups. The 110 °C treated silica had a higher deconvoluted peak ratio than the 750 °C/TMCS treated silica. This finding suggests that 110 °C treated silica forms more hydrogen bonds with the E–Va. As the polymer concentration increases, the hydrogen bonded to non-hydrogen bonded C=O ratio decreases. This suggests that, at a higher polymer concentration, more E–Va molecules are adsorbed and coupled through entanglements instead of direct hydrogen bonds to the silica surface.

Figs 15 and 16 show spectra of E–Va bonded and adsorbed from 2 and 6 vol % polymer solutions onto treated silica surfaces, respectively. There were: (1) three different heat, and (2) three different heat/TMCS treated silica. Fig. 15 shows that on heat treated silica, E–Va forms more hydrogen bonded C=O groups than non-hydrogen bonded C=O groups. On heat/TMCS treated silica, however, it was just the opposite. When E–Va adsorbed from a 2 vol % polymer solution onto heat treated silica, the silica had adequate isolated hydroxyl groups available to form hydrogen bonds. Under this condition, most C=O groups did form hydrogen bonds. In contrast, heat/TMCS treated silica had fewer isolated hydroxyl groups. Fewer hydrogen bonded C=O groups were found at the interface. Accordingly, a higher non-hydrogen bonded C=O peak was observed at 1739 cm^{-1}.

TABLE IV Ratio of hydrogen bonded C–O to non-hydrogen bonded C–O of E–Va on silica surface

Polymer solution concentration (vol %)	Silica treatment	
	110 °C	750 °C/TMCS
0.56[a]	38.50	1.25
0.80	16.45	1.02
4.20[b]	2.74	0.72

[a] Thin coating of E–Va on silica surface.
[b] Thick coating of E–Va on silica surface.

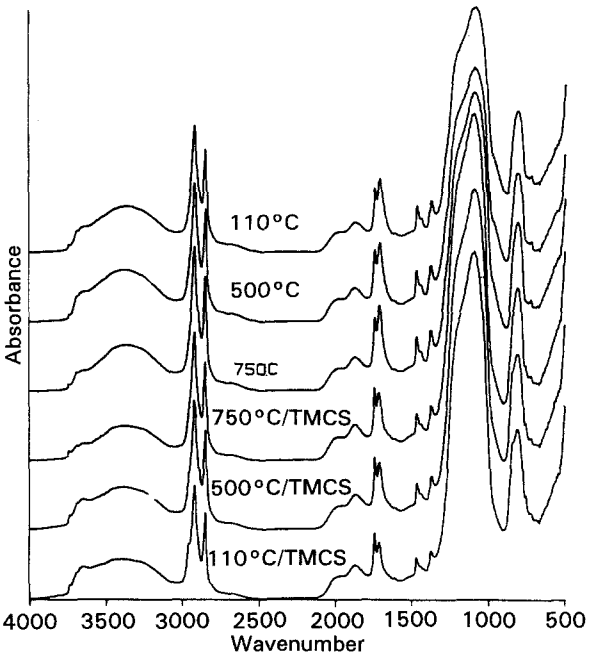

Figure 15 FT-i.r. spectra of E–Va bonded and adsorbed on different Cab-O-Sil silica surfaces from 2 vol % polymer concentrations.

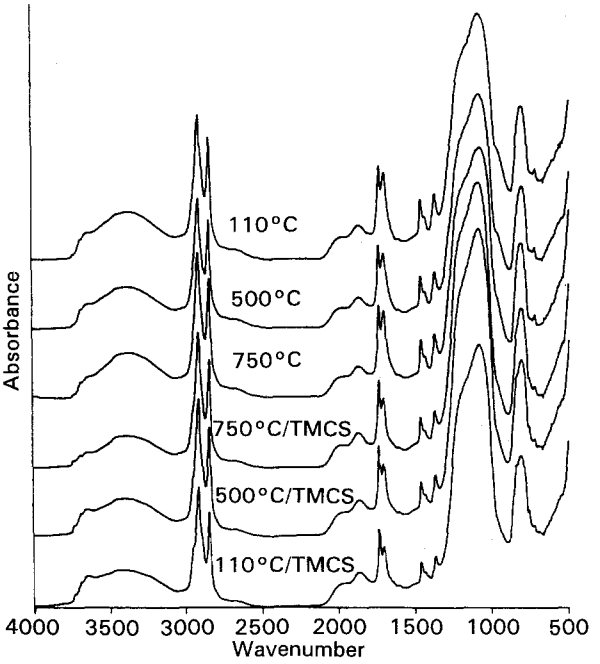

Figure 16 FT-i.r. spectra of E–Va bonded and adsorbed on different Cab-O-Sil silica surfaces from 6 vol % polymer concentrations.

Fig. 16 shows a different C=O peak intensity distribution in a 6 vol % polymer solution. The E–Va contributed with more C=O groups than were available from the isolated hydroxyl groups, which meant that some C=O groups could not form hydrogen bonds. As a consequence, the 1739 cm^{-1} peak was higher than the 1704 cm^{-1} peak regardless of silica surface treatments. The information presented in Figs 15 and 16 is in line with Fig. 12 and Table IV. This fact suggests that more non-hydrogen bonded E–Va molecules are mechanically retained onto the silica surface through entanglement with the bonded polymer when the E–Va molecules are adsorbed from high polymer concentrations.

Fig. 17 shows the relative C=O/Si–O ratio versus polymer volume concentration. This figure suggests that more polymers are bonded and adsorbed as the polymer concentration increases. When polymer was adsorbed from a 6 vol % concentration onto the 110 °C silica, the relative C=O/Si–O ratio was approximately as much as twice that of the 110 °C/TMCS treated silica.

3.9. Quantitative relationship between W_a and interphase thickness

Fig. 18 shows the relative C=O/Si–O versus W_a^{-1} values. The relative C=O/Si–O value correlates with the W_a^{-1} value by a negative slope in the semi-logarithm co-ordinate system. The amount of polymer bonded and adsorbed onto the silica increased with increased W_a, especially at high polymer concentrations.

3.10. W_a on the interphase thickness, Young's modulus, and the tensile strength

It is remarkable that Young's modulus, the tensile strength and the interphase thickness show similar mathematical correlations with W_a. The exponential correlation of the interphase thickness with W_a was similar to those in Young's modulus and the tensile strength. The realtionsips of W_a with respect to Young's modulus, the tensile strength and the interphase thickness suggest that W_a can be used for quantitative evaluations of the interfacial bond strength of composites.

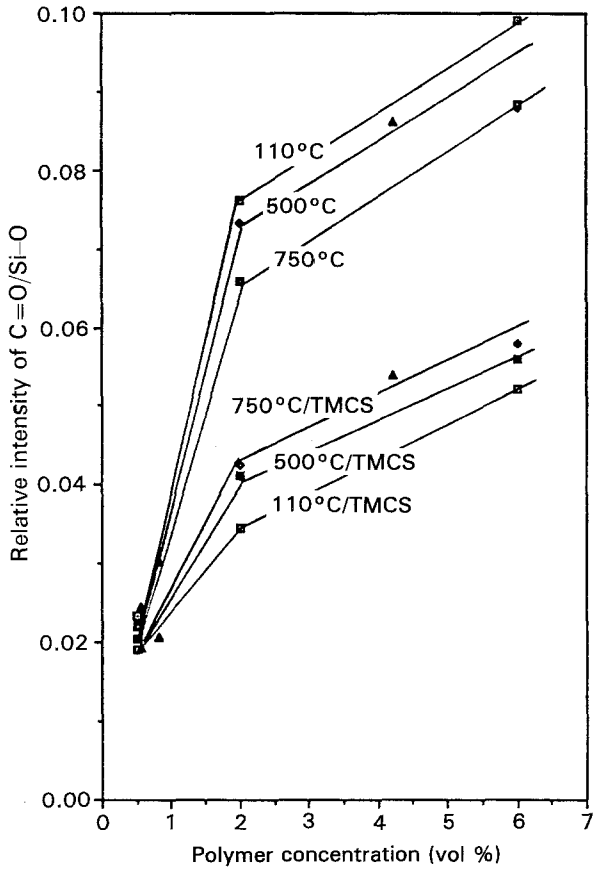

Figure 17 The relative intensity of C = O/Si–O ratio versus polymer concentration vol %. The polymer was adsorbed onto different surface modified silica fillers.

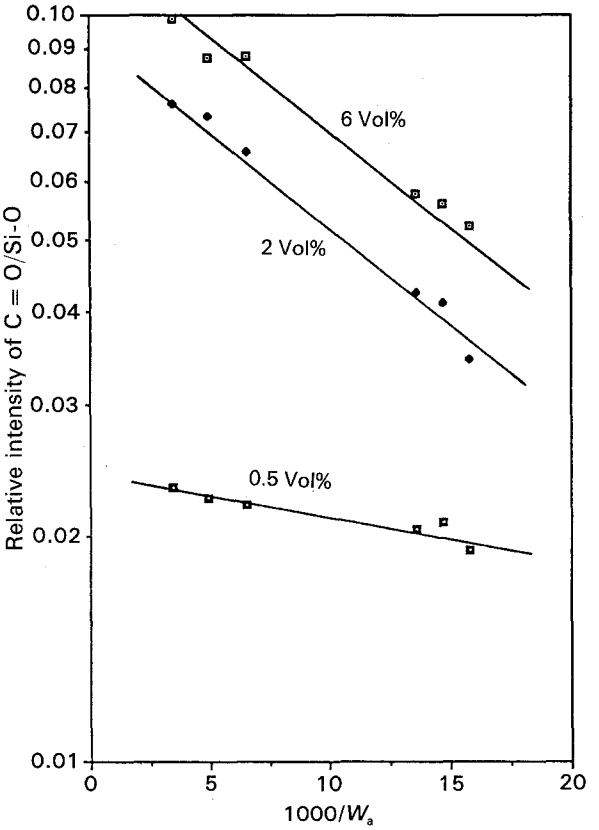

Figure 18 Effect of work of adhesion, W_a, on the relative intensity of C = O/Si–O ratio at different polymer concentrations (□) 6 vol%, (◆) 2 vol %, (■) 0.5 vol %.

4. Conclusions

The findings of this study supports our hypothesis that Young's modulus, the tensile strength and the interphase thickness of particulate filled composites can be correlated with the work of adhesion (W_a) values of their filler particles. These results suggest that the model employed to compute W_a can be used to quantify interfacial bonding. A correlation between interphase thickness and the mechanical properties of silica-filled composites was accomplished.

By increasing the density of hydrogen bonds at the silica filler interface, the W_a value increased. Thus, more polymers were hydrogen bonded on silica surfaces with higher W_a values, which also resulted in a thicker polymer interphase. The hydrogen component of $W_a(W_a^h)$ was the dominant component in predicting Young's modulus, the tensile strength and the interphase thickness of the composites. All three properties correlated similarly with W_a. They all decreased linearly with W_a^{-1} by negative slopes in a semi-logarithmic co-ordinate system. Thus, all three properties increased with increased W_a. The effect of W_a on the tensile strength was dependent on both silica particle size and volume fraction. However, Young's modulus only depended on filler particle size.

For composites filled with Stöber silica with a low W_a value, which means no adhesion, Young's modulus

could be predicted from the Guth–Smallwood equation. As W_a increased, the interphase layer became thicker. This increase in interphase thickness corresponds to an increase in filler fraction, and consequently an increase in Young's modulus. Because of that increase, due to an increase in W_a, an extension of the Guth–Smallwood equation was developed and tested to account for the effect of W_a on Young's modulus.

References

1. S. W. SHANG, J. W. WILLIAMS and K-J. M. SÖDERHOLM, *J. Mater. Sci.* **27** (1992) 4949.
2. K-J. M. SÖDERHOLM and S. W. SHANG, *J. Dent. Res.* **72** (1993) 1050.
3. R. S. CHAHAL and L. E. ST. PIERRE, *Macromolecules* **1** (1968) 152.
4. *Idem, ibid.* **2** (1969) 193.
5. P. H. T. VOLLENBERG and D. HEIKENS, in "Composite interface", edited by H. Ishida and J. L. Koenig (Elsevier Scientific, New York, 1986) p. 171.
6. D. M. BIGG, *Polym. Compos.* **8** (1987) 115.
7. S. MITSUISHI, S. KODAMA and H. KAWASAKI, *ibid.* **9** (1988) 112.
8. A. VOET, *J. Polym. Sci.* **15** (1980) 327.
9. L. E. NIELSEN, in "Mechanical properties of polymer and composites", (Marcel Dekker, New York, 1974) p. 411.
10. M. SUMITA, T. OOKUMA, K. MIYASAKA and K. ISHIKAWA, *J. Appl. Polym. Sci.* **27** (1982) 3059.
11. G. LANDON, G. LEWIS and G. F. BODEN, *J. Mater. Sci.* **12** (1977) 1605.
12. H. ALTER, *J. Appl. Polym. Sci.* **9** (1965) 1525.
13. J. LEIDNER and R. T. WOODHAMS, *Ibid.* **13** (1974) 1639.
14. M. P. WAGNER, in "Additives for plastics", Vol. 2, edited by R. B. Seymou (Academic Press, New York, 1978) p. 25.
15. E. GUTH, *J. Appl. Phys.* **16** (1945) 20.
16. H. M. SMALLWOOD, *ibid.* **15** (1944) 758.
17. J. P. TROTIGNON, B. SANACHAGRIN, M. PIPERAUD and J. VERDU, *Polym. Compos.* **3** (1982) 230.
18. M. E. J. DEKKERS and D. HEIKENS, *J. Appl. Polym. Sci.* **28** (1983) 3809.
19. M. Y. BOLUK and H. P. SCHREIBER, *Polym. Compos.* **7** (1986) 295.
20. F. M. FOWKES and M. A. MOSTAFA, *Ind. Eng. Chem. Prod. Res. Dev.* **17** (1978) 3.
21. F. M. FOWKES, in "Physiochemical aspects of polymer surface", Vol. 2, edited by K. L. Mittal (Plenum, New York, 1983) p. 583.
22. *Idem*, in "Microscopic aspects of adhesion and lubrication", Vol. 7, edited by J. M. Georges (Elsevier, Amsterdam, 1982) p. 119.
23. *Idem*, in "Recent advances in adhesion", edited by L. H. Lee (Gordon & Breach, London, 1973) p. 39.
24. *Idem, J. Adhesion* **4** (1972) 155.
25. F. M. FOWKES, D. C. McCARTHY and D. O. TISCHLER, in "Molecular characterization of composite interface", edited by H. Ishida and G. Kumar (Plenum Press, New York, 1985) p. 401.
26. M. J. MARMO, M. A. MOSTAFA, H. JINNAL and F. M. FOWKES, *Ind. Eng. Chem. Prod. Res. Dev.* **15** (1976) 206.
27. F. M. FOWKES, in "Surface and interfacial aspects of biomedical polymer" Vol. 1, edited by J. D. Andrade (Plenum Press, New York, 1985) p. 337.
28. J. A. MANSON, *Pure & Appl. Chem.* **57** (1985) 1667.
29. J. JANCAR and J. KUCERA, *Polym. Eng. & Sci.* **30** (1990) 707.
30. *Idem, ibid.* **30** (1990) 714.
31. J. A. MANSON and L. H. SPERLING, in "Polymer blend and composites", (Plenum Press, New York, 1981) p. 325.
32. J. W. WILLIAMS, S. W. SHANG and M. D. SACKS, *Mater. Res. Soc. Symp. Proc.* **119** (1988) 17.
33. N. NISHIYAMA, K. HORIE, R. SHICK and H. ISHIDA, *Polym. Com.* **31** (1990) 380.
34. N. C. LIU and W. E. BAKER, *Polym. Eng. & Sci.* **32** (1992) 1695.
35. J. E. SOHN, *J. Adhesion* **19** (1985) 15.
36. J. C. SMITH, G. A. KERMISH and C. A. FENSTERMAKER, *ibid.* **4** (1972) 109.
37. Y. TERMONIA, *J. Mater. Sci.* **25** (1990) 4644.
38. *Idem, ibid.* **27** (1992) 4878.
39. A. FAROUK, N. A. LANGRANA and G. J. WENG, *Polym. Compos.* **13** (1992) 285.
40. W. STÖBER, A. FINK and E. BOHN, *J. Colloid Interface Sci.* **26** (1968) 62.
41. C. G. TAN, B. D. BOWEN and N. EPSTEIN, *ibid.* **118** (1987) 290.
42. R. N. LAMB and D. N. FURLONG, *J. Chem. Soc., Faraday Trans.* **78** (1982) 61.
43. D. K. OWENS and R. C. WENDT, *J. Appl. Polym. Sci.* **13** (1969) 1741.
44. K. TSUTSUMI and H. TAKAHASHI, *Colloid Polym. Sci.* **263** (1985) 506.
45. L. T. ZHURAVLEV, *Langmuir* **3** (1987) 316.
46. J. J. FRIPRAT and J. UYTTERHOEVEN, *J. Phys. Chem.* **66** (1962) 880.
47. O. JOHNSON, *ibid.* **59** (1955) 827.
48. H. A. BENESI, *ibid.* **78** (1956) 5490.
49. *Idem. ibid.* **61** (1957) 970.
50. T. F. TADROS, *J. Colloid Interface Sci.* **64** (1978) 36.
51. E. KILLMANN, J. EISENLAUER and M. KORN, *J. Polym. Sci., Polym. Sympo.* **61** (1977) 413.
52. C. THIES, *J. Phys. Chem.* **70** (1966) 3783.
53. M. HASEGAWA and M. J. D. LOW, *J. Colloid Interface Sci.* **29** (1969) 593.
54. Y. LIPATOV and L. M. SERGEEVA, *Advances in Colloid and Interface Sci.* **6** (1976) 1.
55. J. P. BLITZ, R. S. S. MURTHY and D. E. LEYDEN, *Appl. Spectrosc.* **40** (1986) 829.
56. H. A. BENESI and A. C. JONES, *J. Phys. Chem.* **63** (1959) 179.
57. R. S. SHREEDHARA MURTHY and D. E. LEYDEN, *Anal. Chem.* **58** (1986) 1228.
58. J. L. KOENIG, *Appl. Spectrosc.* **29** (1975) 293.
59. S. R. CULLER, H. ISHIDA and J. L. KOENIG, *Ann. Rev. Mater. Sci.* **13** (1983) 363.
60. M. P. FULLER and P. R. GRIFFITHS, *Anal. Chem.* **50** (1978) 1906.
61. H. MAULHARDT and D. KUNATH, *Appl. Spectrosc.* **34** (1980) 383.
62. R. S. SHREEDHARA MURTHY, J. P. BLITZ and D. E. LEYDEN, *Anal. Chem.* **58** (1986) 3167.
63. T. HATTORI, K. SHIRAI, M. NIWA and Y. MURAKAMI, *Bull. Chem. Soc. Jpn.* **54** (1981) 1964.
64. D. E. LEYDEN, R. S. SHREEDHARA MURTHY and J. P. BLITZ, *Appl. Spectrosc.* **41** (1987) 920.
65. M. L. HAIR, in "Infrared spectroscopy in surface chemistry", (Marcel Dekker, New York. 1967) p. 79.
66. *Idem*, in "Silanes, surfaces, and interfaces symposium, Snowmass, CO, 1985", edited by D. E. Leyden (Gordon and Breach Sci., Amsterdam, 1986) p. 25.
67. M. L. HAIR and W. HERTL, *J. Phys. Chem.* **73** (1969) 2372.
68. B. EVANS and T. E WHITE, *J. Catalysis* **11** (1968) 336.
69. W. HERTL, *J. Phys. Chem.* **72** (1968) 1248.
70. *Idem, ibid.* **72** (1968) 3993.
71. F. M. FOWKES, D. O. TISCHLER, J. A. WOLFE and M. J. HALLIWELL, *Org. Coating Appl. Polym. Sci. Proc.* **46** (1982) 1.
72. G. KRAUS, *Rubber Chem. Technol.* **38** (1964) 1070.
73. M. P. WAGNER, *ibid.* **49** (1976) 703.
74. D. PARKINSON, in "Reinforcement of rubber" (Lakeman, London, 1957) p. 14.

Received 12 January 1993
and accepted 31 August 1993